Journal of Alloys and Compounds 504S (2010) S65–S68

Contents lists available at ScienceDirect

Journal of Alloys and Compounds

journal homepage: www.elsevier.com/locate/jallcom

Serrated flow and shear band evolution in a Zr-based bulk metallic glass after plastic deformation and annealing

J.S. Gu[a], B.C. Wei[a,*], T.H. Zhang[b], Y.H. Feng[b], Z.W. Sun[a]

[a] Key Laboratory of Microgravity (National Microgravity Laboratory), Institute of Mechanics, Chinese Academy of Sciences, Beijing 100190, PR China
[b] State Key Laboratory of Nonlinear Mechanics (LNM), Institute of Mechanics, Chinese Academy of Sciences, Beijing 100190, PR China

ARTICLE INFO

Article history:
Received 5 August 2009
Received in revised form 13 January 2010
Accepted 8 February 2010
Available online 12 February 2010

Keywords:
Bulk metallic glass
Deformation
Annealing
Shear bands

ABSTRACT

The effect of pre-deformation and annealing on serrated plastic flow and shear band features of a Zr-based bulk metallic glass was investigated through nanoindentation and macroindentation tests. The results showed that the serrated plastic flow during the loading process of nanoindentation was significantly suppressed in pre-deformed sample and re-appeared after subsequent annealing. The effect of pre-existed shear bands on the development of final shear bands was characterized by macroindentation without bonded interfaces. Pre-deformation does not lead to the multiply of shear band during the consequent plastic deformation, but decrease the shear band number significantly. The change in plastic flow behavior of the alloy by pre-deformation is thought to be the preferential propagation of existed shear bands, and its effect can be eliminated by annealing below glass transition temperature.

1. Introduction

Bulk metallic glasses (BMGs) have received considerable interests since the early 1990s due to their unique physical, chemical and mechanical properties being of special interest for a wide range of potential applications [1–3]. However, BMGs display little or no plastic deformation at room temperature because the plastic flow in a BMG is governed by the formation of localized shear bands [4,5]. To overcome this problem, many researchers have made attempts to develop an extrinsic composite microstructure within the glassy matrix [6,7], or an intrinsic structure such as BMGs with high Possion's ratio or with large free volume [8–10]. Recently, "work-ductilizing" phenomenon has been reported in BMGs through cold rolling [11,12], pre-compression [13], surface shot-peening [14] or high pressure pre-treatment [15]. The ductility improvement might be related to more uniform deformation induced by a high population of pre-existing shear bands.

It is well known that pre-plastic deformation makes crystalline metals stronger and harder because dislocations nucleate and multiply during the plastic deformation. In contrast, pre-strain generally soften the BMGs due to the increase of free volume with respect to the un-deformed sample [16]. However, pre-deformation might also strengthen the BMGs, because of the strain-induced structural heterogeneity or nanocrystallization [17]. Jiang et al. [18] found that cold rolling could reduce the amplitude of strain serrations in the load–displacement curve, while Bhowmick et al. [19] found that pre-plastic deformation could enhance the serrations in the plastically pre-deformed region. It is evident that more work should be done for further understanding the underlying mechanism of effect of pre-existed shear bands induced on the final deformation behavior in BMGs.

In this work, a ductile $Zr_{64.13}Cu_{15.75}Ni_{10.12}Al_{10}$ [9] BMG was pre-strained up to 53% by constrained compression. The effect of the pre-strain on the shear banding feature and shear band pattern during consequent loading was characterized by multi-scale indentation measurements. In order to further understanding mechanical response of a pre-strained BMG, the pre-strained and as-cast samples were also annealed below glass transition temperature for comparisons.

2. Experimental procedures

The alloy ingots of $Zr_{64.13}Cu_{15.75}Ni_{10.12}Al_{10}$ were first prepared by arc-melting a mixture of pure Zr, Cu, Ni, and Al metals with purities higher than 99.9% under an argon atmosphere. In order to obtain the homogeneity, the alloy ingots were re-melted several times before cast into a water-cooled copper mold using an in situ suction-casting facility. The resulting cylindrical BMG rods have a dimension of 5 mm in diameter and 100 mm in length. Pre-strain treatment was conducted on the as-cast short rods with an aspect ratio of about 0.64 (ϕ5 mm × 3.2 mm) through a standard Instron testing machine at strain rates of $1 \times 10^{-4}\,s^{-1}$. The specimen was plastically compressed by a plastic strain of about 53%. Both as-cast and pre-deformed samples were annealed at 590 K which is lower than the glass transition temperature for 6 h. The structures of the samples obtained were examined by X-ray diffraction (XRD) with Cu Kα radiation. The thermal response of all alloys was investigated with differential-scanning calorimetry (DSC, NETZSCH DSC-404C) at a heating rate of 20 K/min in an argon atmosphere.

* Corresponding author. Tel.: +86 10 82544118; fax: +86 10 82544096.
E-mail address: weibc@imech.ac.cn (B.C. Wei).

0925-8388/$ – see front matter © 2010 Elsevier B.V. All rights reserved.
doi:10.1016/j.jallcom.2010.02.021

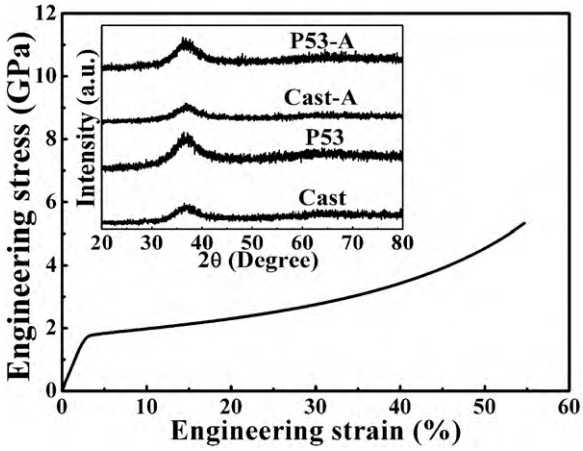

Fig. 1. Engineering stress–strain curve for the constrained compression of as-cast specimen with small aspect ratio at the initial strain rate of $1.0 \times 10^{-4}\ s^{-1}$. The insets are XRD patterns of the four specimens at various states.

The specimens for indentation measurements were mechanically polished to a mirror finish. Nanoindentation measurements were carried out in an MTS Nano-Indenter XP fitted with a Berkovich indenter. A load control mode to a depth limit of 1 μm was employed. Shear band pattern of the sample at various states was characterized through Rockwell hardness tester with the static load 1500 N and the dwell time of loading was 15 s. The deformation morphology around the indents after indentation was studied by scanning electron microscopy (SEM) and optical microscope (OM).

3. Results and discussion

The typical engineering stress–strain curve during the pre-deformation of the as-cast rods with the aspect ratio of about 0.64 is shown in Fig. 1. The smooth stress–strain curve implies a macroscopically homogeneous plastic deformation in the specimen [20]. XRD patterns of the as-cast (Cast), as-cast plus annealing (Cast-A), pre-deformed (P53), and pre-deformed plus annealing (P53-A) specimens are shown in the inset of Fig. 1. The broad diffraction maxima demonstrate that the specimens at various states are all of amorphous structure. The severely plastic deformation and the subsequent annealing did not cause detectable crystallization.

DSC thermograms of the four amorphous alloys are shown in Fig. 2. It can be seen that the onset crystallization temperature (T_x) of the alloy does not change distinctly upon the pre-deformation, annealing or pre-deformation plus annealing treatments. Moreover, the annealed and pre-deformation plus annealed specimens exhibit an almost identical DSC trace, with an endothermic overshoot at the beginning of glass transition. Whereas, a broad exothermic peak can be found in the DSC traces of the as-cast and pre-deformed specimens below glass transition temperature (T_g). The area of the exothermic peak increases from 8 J/g for the as-cast specimen to 13 J/g for the 53% plastically deformed specimen. The T_g, T_x, and the exothermic enthalpy of the four specimens are list in Table 1. Van de Beukel and Sietsma [21] proposed that prior to T_g, the exothermic event strongly links with the existence of free volume in BMGs, which was testified by Slipenyuk and Eckert [22]. This indicates that the pre-deformed sample has more free volume or atomic-scale defects than the as-cast sample because of pre-existing shear bands. However, after annealing at temperature 590 K for 6 h, both the annealed as-cast sample and annealed pre-deformed sample have almost identical DSC curves. This means that the pre-existing shear bands have been recovered by annealing and the structure of annealed pre-deformed sample is almost identical to the annealed as-cast sample.

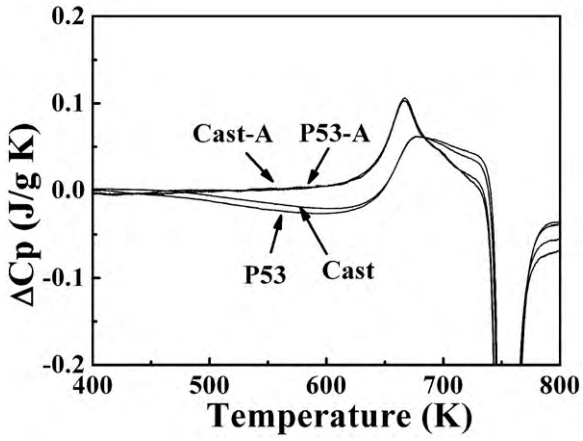

Fig. 2. The DSC curves of the four specimens.

Table 1
Thermal and mechanical properties of the BMGs at various states (Cast: as-cast specimen; P53: pre-deformed specimen; Cast-A: annealed Cast; P53-A: annealed P53).

Specimen	T_g (K)	T_x (K)	ΔH (J/g)	H (GPa)	E (GPa)
Cast	645	746	8	5.90 ± 0.09	93.10 ± 1.73
P53	645	746	13	5.81 ± 0.14	91.22 ± 1.19
Cast-A	650	744	0	6.17 ± 0.20	101.45 ± 1.20
P53-A	650	744	0	6.16 ± 0.11	101.03 ± 2.29

To examine the effect of this pre-existing shear bands and the recovery of them on the plastic deformation behavior of the $Zr_{64.13}Cu_{15.75}Ni_{10.12}Al_{10}$ BMGs, instrumental nanoindentations were carried out on the four specimens. The hardness and elastic modulus obtained from the P–h curves of nanoindentation are

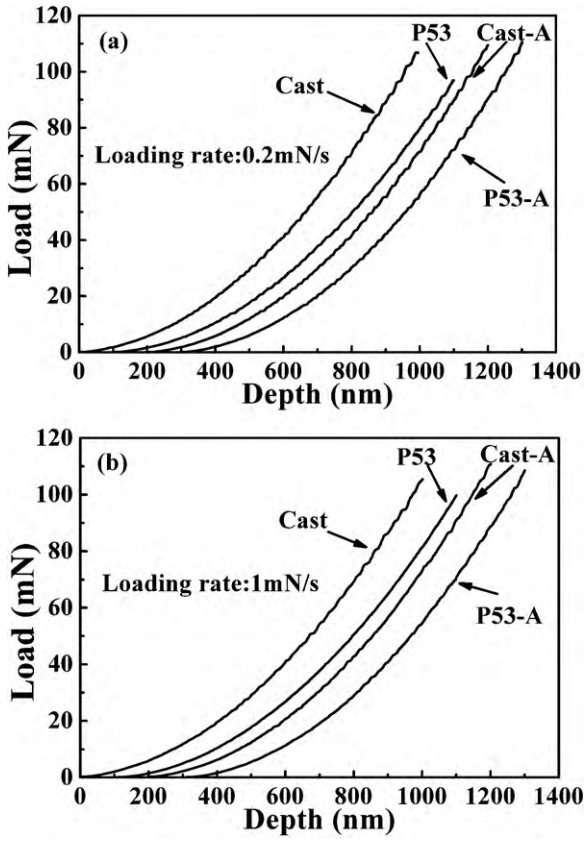

Fig. 3. Typical load–depth (P–h) curves of the four samples during nanoindention at loading rates of 0.2 mN/s (a) and 1 mN/s (b).

also listed in Table 1. It is shown that the pre-deformed specimen has the average hardness of 5.81 GPa and modulus of 91.22 GPa respectively, which are about 2% lower than the values of the as-cast specimen. However, the scatter in the hardness data for the P53 specimen (2.4%) is larger than that in the as-cast one. This indicates that pre-deformation leads to a local softening of the BMG, owing to the introduction of excess free volume or atomic-scale defects, though few pre-existed shear bands are involved in the small plastic deformation region during nanoindentation. This consists with previous results, wherein a lower hardness was observed in the pre-deformed region [16]. In contrast, annihilation of free volume or atomic-scale defects during annealing increases the hardness and modulus of the as-cast specimen significantly by about 5% and 9%, respectively. It should be noted that annealing the pre-deformed specimen gives rise to almost same values of hardness and modulus as the annealed as-cast specimen. This further supports the idea that the excess free volume or atomic-scale defects induced by the pre-deformation could be completely annihilated by annealing below T_g.

Typical load–depth (P–h) curves of the four samples at the loading rates of 0.2 and 1 mN/s are shown in Fig. 3. The origin of each curve is displaced for clear observation. Serrated flow phenomenon can be observed during the loading process of nanoindentation for all samples, and is less obvious at high loading rate as in other Zr-based BMGs [23]. Annealing at 590 K for 6 h does not distinctly change the serrated flow of the as-cast specimen. It is worth noting that the serrated flow in the pre-deformed specimen is weaker than that in the as-cast sample, especially at the loading rate of 1 mN/s. This indicates that the pre-existed shear bands do affect the deformation behavior of the BMG during nanoindentation, though the plastic deformation region of nanoindentation is quite small (with a depth of about 5 μm in the present case). It can also be seen that annealing recovers the serrated flow phenomenon of the pre-deformed specimen, and gives rise to a strain serration magnitude similar to that of the as-cast specimen.

For understanding the effect of pre-deformation and annealing on the plastic deformation behavior of the BMG, Rockwell indentation tests were used to characterize the plastic deformation region feature of the four samples. Fig. 4 shows the typical upper surface morphologies around the indents for the four samples after indentation under the load of 1500 N. Well developed shear band pattern can be found around the indents for all samples. The shear bands originate at the edge of the indent following an outward logarithmic spiral pattern. It should be noted that the shear band pattern in the pre-deformed specimen (Fig. 4c) is quite different from that in the as-cast specimen (Fig. 4a). Shear bands are rough and irregular in the pre-deformed specimen in contrast to the regular and smooth shear bands in the as-cast specimen. Moreover, the shear band spacing at the edge of the indents in the pre-deformed specimen is about 25 μm, which is about twice larger than that of the as-cast specimen. The shear bands spacing here (about 25 μm) is comparable to that of a similar BMG uniaxially compressed by about 50% plastic strain [16]. The much less shear band number in the pre-deformed specimen indicates that the plastic deformation during the indentation is governed by the propagation of the pre-existing shear bands, rather than the nucleation of new shear bands. During indentation shear band first forms along the pre-existed shear band, and its further propagation will cause the shear band deviate significantly from the maximum shear stress plane. Then the propagation along existed shear band stops, and new shear bands along the maximum shear plane forms, until it meets another pre-existed shear band. This kind of movement of shear bands leads to the irregular and tough shear band pattern in the pre-deformed specimen, and its much less shear band number is due to the contribution of pre-existed shear bands on the final plastic deformation. The weakness of serrated flow during nanoindentation in the pre-deformed specimen may also related to the preferential propagation of shear bands along the pre-existed shear bands, which is deviated from the maximum shear plane. Annealing at 590 K for 6 h does not distinctly change the shear band pattern of the as-cast specimen. Whereas,

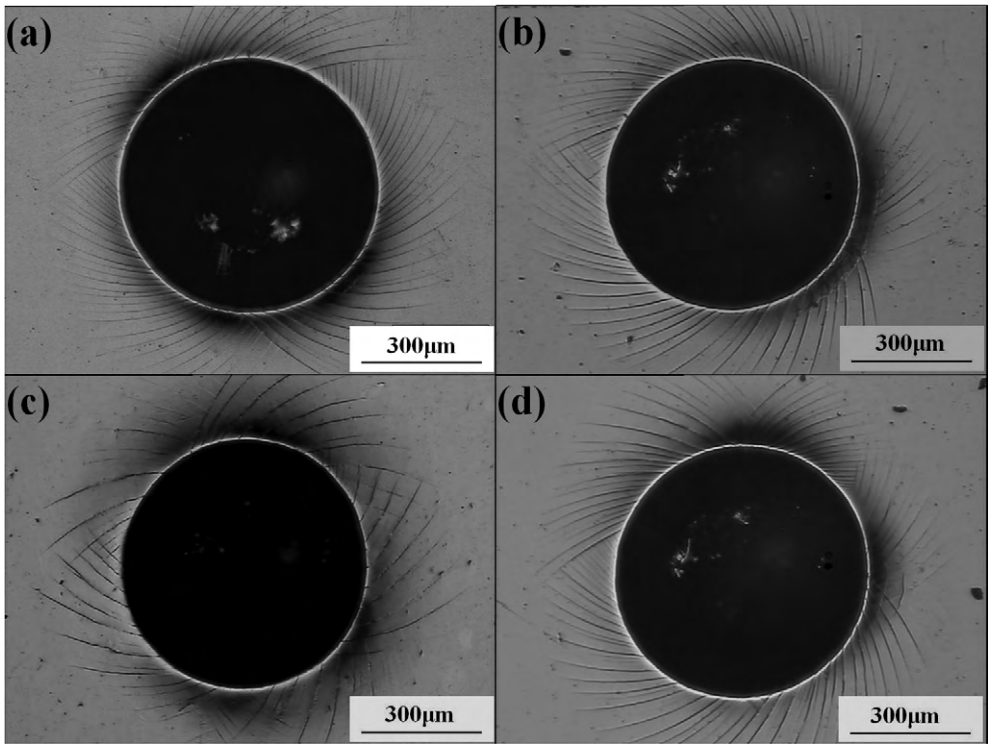

Fig. 4. Shear band morphologies around indents after Rockwell indentation of $Zr_{64.13}Cu_{15.75}Ni_{10.12}Al_{10}$ BMG at various states: (a) Cast; (b) Cast-A; (c) P53; (d) P53-A.

in the pre-deformation plus annealing sample, the shear bands are again smooth and regular, with the shear band spacing similar to the as-cast (Fig. 4a) and the annealed specimens (Fig. 4b). This further proves that annealing below T_g can eliminate the effect of the pre-existed shear bands.

4. Conclusions

The effect of pre-deformation and annealing on mechanical behavior and shear band pattern of a $Zr_{64.13}Cu_{15.75}Ni_{10.12}Al_{10}$ BMG was studied by multi-scale indentation tests. Pre-deformation leads to the local softening and weaker serrated flow phenomenon during nanoindentation of the BMG. This is related to the preferential propagation of shear bands along the pre-existed shear bands, which is confirmed by the rough and much less shear bands after macroindentation of the pre-deformed specimen. This effect of pre-deformation on the consequent plastic deformation can be eliminated completely by annealing the specimen below glass transition temperature.

Acknowledgements

This work is financially supported by the National Nature Science Foundation of China (Grant Nos. 50731008 and 50771102) and National Basic Research Program of China (973 Program, No. 2007CB613905).

References

[1] W.L. Johnson, MRS Bull. 24 (1999) 42–56.
[2] A. Inoue, Acta Mater. 48 (2000) 279–306.
[3] M.F. Ashby, A.L. Greer, Scripta Mater. 54 (2006) 321–326.
[4] F. Spaepen, Acta Metall. 25 (1977) 407–415.
[5] A.S. Argon, Acta Metall. 27 (1979) 47–58.
[6] C.C. Hays, C.P. Kim, W.L. Johnson, Phys. Rev. Lett. 84 (2000) 2901–2904.
[7] D.C. Hofmann, J.Y. Suh, A. Wiest, et al., Nature 451 (2008) 1085–1089.
[8] J. Schroers, W.L. Johnson, Phys. Rev. Lett. 93 (2004) 255506.
[9] Y.H. Liu, G. Wang, R.J. Wang, et al., Science 315 (2007) 1385–1388.
[10] L.Y. Chen, et al., Phys. Rev. Lett. 100 (2008) 075501.
[11] Y. Yokoyama, K. Yamano, K. Fukaura, et al., Mater. Trans. 42 (2001) 623–632.
[12] Y. Yokoyama, K. Inoue, K. Fukaura, Mater. Trans. 43 (2002) 3199–3205.
[13] L. He, M.B. Zhong, Z.H. Han, et al., Mater. Sci. Eng. A 496 (2008) 285–290.
[14] Y. Zhang, W.H. Wang, A.L. Greer, Nat. Mater. 5 (2006) 857–860.
[15] P. Yu, H.Y. Bai, J.G. Zhao, et al., Appl. Phys. Lett. 90 (2007) 051906.
[16] H. Bei, S. Xie, E.P. George, Phys. Rev. Lett. 96 (2006) 105503.
[17] Q.P. Cao, J.F. Li, Y. Hu, et al., Mater. Sci. Eng. A457 (2007) 94–99.
[18] W.H. Jiang, F.E. Pinkerton, M. Atzmon, Acta Mater. 53 (2005) 3469–3477.
[19] R. Bhowmick, R. Raghavan, K. Chattopadhyay, et al., Acta Mater. 54 (2006) 4421–4428.
[20] K. Mondal, G. Kumar, T. Ohkubo, et al., Philos. Mag. Lett. 87 (2007) 625–635.
[21] A. van den Beukel, J. Sietsma, Acta Metall. Mater. 38 (1990) 383–389.
[22] A. Slipenyuk, J. Eckert, Scripta Mater. 50 (2004) 39–44.
[23] C.A. Schuh, T.G. Nieh, Acta Mater. 51 (2003) 87–99.